Anal Bioanal Chem (2016) 408:295–305
DOI 10.1007/s00216-015-9108-1

RESEARCH PAPER

A direct solid sampling analysis method for the detection of silver nanoparticles in biological matrices

Nadine S. Feichtmeier[1] · Nadine Ruchter[2] · Sonja Zimmermann[2] · Bernd Sures[2] · Kerstin Leopold[1]

Received: 24 August 2015 / Revised: 6 October 2015 / Accepted: 8 October 2015 / Published online: 19 October 2015

Abstract Engineered silver nanoparticles (AgNPs) are implemented in food contact materials due to their powerful antimicrobial properties and so may enter the human food chain. Hence, it is desirable to develop easy, sensitive and fast analytical screening methods for the determination of AgNPs in complex biological matrices. This study describes such a method using solid sampling high-resolution continuum source graphite furnace atomic absorption spectrometry (GFAAS). A recently reported novel evaluation strategy uses the atomization delay of the respective GFAAS signal as significant indicator for AgNPs and thereby allows discrimination of AgNPs from ionic silver (Ag^+) in the samples without elaborate sample pre-treatment. This approach was further developed and applied to a variety of biological samples. Its suitability was approved by investigation of eight different food samples (parsley, apple, pepper, cheese, onion, pasta, maize meal and wheat flour) spiked with ionic silver or AgNPs. Furthermore, the migration of AgNPs from silver-impregnated polypropylene food storage boxes to fresh pepper was observed and a mussel sample obtained from a laboratory exposure study with silver was investigated. The differences in the atomization delays (Δt_{ad}) between silver ions and 20-nm AgNPs vary in a range from −2.01±1.38 s for maize meal to +2.06±1.08 s for mussel tissue. However, the differences were significant in all investigated matrices and so indicative of the presence/absence of AgNPs. Moreover, investigation of model matrices (cellulose, gelatine and water) gives the first indication of matrix-dependent trends. Reproducibility and homogeneity tests confirm the applicability of the method.

Keywords Silver nanoparticle detection · Direct solid sampling · Graphite furnace atomic absorption spectrometry · Silver nanoparticle entry in food · Biological samples · Robust screening method

Introduction

Nanotechnology is nowadays a highly active research area and has found numerous applications also in consumer products. Especially, silver nanoparticles (AgNPs) are widely used because of their antimicrobial properties and relatively low cost. Fields of application include amongst others cosmetics, wall paints, textiles, laundry detergents, biocide sprays, sport clothes and medical devices. In the food industry, AgNPs are used for new packaging materials with improved antimicrobial properties and have been commercially available for many years [1, 2]. In contrast to other plastic additives, like phthalates and brominated flame retardants, AgNPs are not covalently bound to the plastic matrix and thus may be released during use [2]. In fact, numerous studies recently showed that silver has the potential to migrate from the packaging into food and/or food simulants under various experimental conditions [3–9]. It was stated in all reports that a proportion of the migrated silver was in nanoparticle form; hence, AgNPs are thereby entering the human food chain. For this reason, the Scientific Committee of the European

Electronic supplementary material The online version of this article (doi:10.1007/s00216-015-9108-1) contains supplementary material, which is available to authorized users.

✉ Kerstin Leopold
kerstin.leopold@uni-ulm.de

[1] Institute of Analytical and Bioanalytical Chemistry, University of Ulm, Albert-Einstein-Allee 11, 89077 Ulm, Germany

[2] Institute of Aquatic Ecology, University of Duisburg-Essen, Universitätsstr. 5, 45141 Essen, Germany

Food Safety Authority (EFSA) published in 2009 a scientific opinion on nanoscience and nanotechnologies in relation to food and feed safety [10]. According to the scientific opinion of EFSA, the migration of Ag should not exceed a maximum level of 0.05 mg per kg food [11]. Furthermore, a recent regulation in the European Union requires food ingredients to be identified when they are present in the nanoform [12]. Enforcement of this directive will inevitably also require checking foodstuff that comes into contact with packaging materials for the presence of AgNPs, even though there is currently no legislation to detect AgNPs in food and feed [10, 13, 14].

Hence, there is a need for valid and robust analytical methods to determine AgNPs in biological matrices. However, methods for the separation, identification, characterization and quantification of nanomaterials in consumer products, food and environmental samples are still limited due to low concentrations and complexity of the sample matrices. Most approaches are elaborative multi-step procedures that include (partial) digestion or decomposition of the matrix and selective separation of NPs prior to element-specific instrumental detection [15–20]. In some cases, unintended transformation of AgNPs during multi-step sample pre-treatment procedures may cause biased results impairing the validity of the obtained data [21]. For the detection of AgNPs in cell culture medium [22], chicken meat [23] and colloidal silver-based consumer products [24], asymmetric flow field-flow fractionation coupled to inductively coupled plasma mass spectrometry (AF^4-ICP-MS) after respective sample preparation has been successfully applied. Recently, the use of ICP-MS operating in single-particle mode (spICP-MS) has been suggested in order to obtain the size distribution of AgNPs in liquid samples without prior chromatographic separation [23, 25]. This approach was recently tested in a round robin test for its applicability to food samples, and the authors of the study declared the method as a very promising tool in this regard [26]. In a pioneering study performed by Gagné et al. [27], a distinction of AgNPs from silver ions in acidified homogenates of the liver of rainbow trout was achieved using graphite furnace atomic absorption spectrometry (GFAAS) and interpretation of the signals at different atomization temperatures. This was the first report on NP identification using an AAS technique.

However, all these methods require sample preparation by means of dissolution/decomposition of solid matrices and transferring the analyte (AgNPs) into a liquid sample. Accordingly, long analysis times arise causing high costs and making these procedures less attractive for monitoring purposes. Consequently, the development of direct methods for the qualitative investigation of large sample series as a fast screening tool is very meaningful. In this regard, high-resolution continuum source graphite furnace atomic absorption spectrometry (HR-CS SS GFAAS) has shown great potential in direct analysis of solid samples in a broad variety of analytical questions in recent years [28]. Several studies have proven its suitability for the direct determination of Ag in solid biological material, e.g. in *Daphna magna* specimens [29] or mice tissue [30] after exposition to AgNPs. However, these studies focussed on the direct determination of total silver rather than on distinction of AgNPs and ionic Ag species. For the discrimination of AgNPs and ionic Ag (silver salts) in solid samples by direct HR-CS SS GFAAS, a novel approach has been suggested recently by our group [31]. Detection of AgNPs and their direct discrimination from ionic Ag in dried parsley was achieved by the development of a novel evaluation strategy that applies the atomization delay of the signal as significant indicator for AgNPs. Nanoparticles in a size range from 20 to 80 nm were investigated and could all be clearly distinguished from ionic silver in spiked parsley samples. The difference in atomisation delay was ascribed to a much stronger interaction of ionic silver (Ag^+) ions with the biological matrix than AgNPs. It was suggested that a low pre-treatment temperature in the graphite furnace results in incomplete degradation of the biological matrix and so slows down the evaporation and atomisation of Ag^+ ions. In the present study, further development of this method was performed and its suitability was investigated for nine different biological matrices (parsley, apple, pepper, cheese, onion, pasta, maize meal, wheat flour and mussel tissue), which were either spiked with ionic Ag or AgNPs or obtained from exposure studies. Furthermore, the reproducibility of the developed solid sampling method was assessed by replicate measurements using different sampling tubes and platforms.

Materials and methods

Instrumentation

For high-resolution continuum source atomic absorption spectrometry (HR-CS AAS), a contrAA 600 spectrometer, commercially available from Analytik Jena (Jena, Germany) was used. The instrument is equipped with a graphite furnace atomization unit and an SSA 600 auto sampler for solid sampling. Pyrolytic graphite-coated solid sampling tubes without dosing holes (Analytik Jena AG, no. 407-A81.303) have been used throughout. Samples were weighed on a M2P microbalance (Sartorius, Göttingen, Germany) and inserted into the graphite tubes on pyrolytic graphite-coated SS platforms (Analytik Jena AG, no. 407-152.023), using a pre-adjusted set of tweezers, which is part of the SSA 5 accessory for solid sampling. Argon with a purity of 99.999 % (MTI, Neu-Ulm, Germany) was used as purge and protective gas. Data evaluation was achieved with the ASpect CS 2.0.0 software. The most sensitive Ag line at 328.07 nm has been used for atomic absorption of silver. Atomic absorption was measured using

centre pixel no. 101 and centre pixel ±1. The background was corrected by iterative baseline correction (IBC) algorithm. The graphite furnace temperature programme applied in a previous study [31] for identifying AgNPs in parsley samples was further optimized for pyrolysis and atomization temperature as well as for atomization heating rate and sample weight. Achieved optimal parameters are presented in Table 1.

Chemicals

All solutions were prepared using purified water obtained from a Milli-Q system (Millipore, Billerica, USA). For acidification, sample digestion and extraction, 65 % nitric acid (HNO_3; p.a., Merck, Darmstadt, Germany) was used. For the preparation of silver-spiked model and food samples, either silver standard solution ($AgNO_3$ in 2 % *w/w* HNO_3, *c* (Ag)=1000 mg L^{-1}; Sigma-Aldrich, St. Louis, USA) or citrate-stabilized silver nanoparticle dispersions of declared size (20 nm) and concentration (5 mg L^{-1}) supplied from BBI Solutions (Cardiff, UK) were used. All reagents were applied without any pre-treatment or further purification.

Samples and sample preparation

Spiked food samples Eight different food samples that were originally not in contact with AgNP-containing packaging material, namely fresh apple, cheese, onion, parsley and red pepper as well as dried noodles, maize meal and wheat flour, were purchased in a local supermarket. Fresh food was first chopped using a pre-cleaned and disinfected kitchen knife and dried to constant mass for 24 h at 80 °C. All dried samples were pestled in an achate mortar to obtain homogenous powder samples. In addition, two model matrices, namely pure cellulose (powder; Sigma-Aldrich, St. Louis, USA) and gelatine (reagent grade; AMRESCO, Solon, USA), were commercially purchased in powder form.

For preparation of Ag-spiked samples, which were used for method optimization and proof of concept, 0.3 mg of these fine-grained homogenized samples were spiked with Ag by addition of either 2 mL of 100 μg L^{-1} 20-nm AgNPs or 100 μg L^{-1} Ag^+ standard solution, respectively. The obtained slurry was mixed thoroughly and then placed in a drying oven at 80 °C for about 24 h until complete dehydration. The obtained Ag-spiked solids were all milled again manually with an agate mortar to obtain a powder-like product.

The total silver content was determined after digestion of about 8.4 mg of the sample in 90 μL of 65 % HNO_3 heating up to 95 °C for 30 min in a water bath. The resulting digests were allowed to cool down to room temperature, before analysis by HR-CS GFAAS using the recommended programme of the instrument's supplier for Ag determination in liquid samples after calibration in a range from 10 to 90 μg L^{-1}. The Ag concentrations in the spiked samples ranged from 0.225±0.022 to 0.729±0.011 μg g^{-1} (see Electronic Supplementary Material Table S1). Moreover, their homogeneity was evaluated by calculating the homogeneity factor (H_e) according to Kurfürst et al. [32] using Eq. (1).

$$H_e = \mathrm{RSD}\cdot\sqrt{m} \quad (1)$$

where

H_e	homogeneity factor
RSD	relative standard deviation
m	mean sample mass

Contact sample AgNP-containing food contact material, i.e. nanosilver-impregnated polypropylene (PP) boxes, was purchased (CLOC; Neoflam, Mullumbimby, Australia). First, the presence of Ag in the purchased boxes was approved by extracting Ag into 65 % HNO_3 for up to 7 days at room temperature (see Electronic Supplementary Material Fig. S1). To study the potential transfer of Ag into a food sample, chopped fresh red pepper was stored for up to 7 days at room temperature or at 4 °C, respectively, in these boxes. After deposition, the samples were dried, homogenized and investigated by the newly developed direct HR-CS SS GFAAS method.

Exposure sample The sample was derived from an exposure study performed at the Institute of Aquatic Ecology, University of Duisburg-Essen, Germany, in which zebra mussels (*Dreissena polymorpha*, length between 18 and 25 mm) were maintained in plastic tanks (20 L) with reconstituted water (preparation according to [33]) and exposed to 500 μg Ag L^{-1} using either $AgNO_3$ (ICP standard solution, 1 g Ag L^{-1}; Bernd Kraft GmbH, Duisburg, Germany) or 75-nm PVP-coated AgNPs (assembled by the Institute of Inorganic Chemistry, University of Duisburg-Essen, Germany; for details, see [34]). The general procedure for mussel exposure and harvesting can be found in detail elsewhere [35]. Briefly, after 7 days of exposure, 20 mussels were transferred to clean water not containing silver for 24 h to remove loosely attached metals from the mussel surfaces and killed by deep freezing (−20 °C). Subsequently, mussels were thawed at room temperature and their soft tissues were merged into one sample, homogenized with a dispersing tool (Ultra Turrax T25; Janke & Kunkel, Staufen, Germany) and freeze-dried (Heto PowerDry LL3000, Thermo, Langenselbold, Germany). The dried mussel tissue was then investigated using the new developed direct HR-CS SS GFAAS method.

Interpretation of HR-CS SS GFAAS measurement data

Other than in the common interpretation of GFAAS data here, the signals were evaluated with respect to the time delay for

Table 1 Optimized parameters for graphite furnace programme for direct detection of AgNPs in food samples by means of HR-CS SS GFAAS by applying 0.2-mg-weight sample

Step	Temperature (°C)	Heating rate (°C s^{-1})	Hold time (s)
Drying I	80	5	20
Drying II	130	10	20
Pyrolysis	250	300	20
Auto-zero	250	0	5
Atomization	900	1200	20 (or 30 for mussel)
Cleaning	2500	500	4

maximum absorbance. This strategy has been described in detail in our previous study [31]. Briefly, the time from setting the graphite furnace to atomisation temperature until the maximum peak for absorbance appeared was measured (atomisation delay in s; t_{ad}). The difference in t_{ad} for samples containing Ag^+ ions and those containing AgNPs as calculated by Eq. (2) was defined as Δt_{ad}:

$$\Delta t_{ad} = t_{ad}(Ag^+) - t_{ad}(AgNPs) \quad (2)$$

where

Δt_{ad} difference in atomization delay in seconds
t_{ad} atomization delay in seconds

For Δt_{ad}, the uncertainty was estimated by calculating the relative combined uncertainty (u_c) according to Eq. (3).

$$u_c = \sqrt{RSD^2(t_{ad}(Ag^+)) + RSD^2(t_{ad}(AgNPs))} \quad (3)$$

where

u_c relative combined uncertainty in percent
RSD relative standard deviation

With the optimization of graphite furnace temperature programme and sample weight, t_{ad} values were significant ($p \leq 0.05$) without normalizing to the sample weight (as performed in our previous study).

Results and discussion

Optimization of direct solid sampling method

In a recently published study of our group, it was shown that AgNPs can be identified and distinguished from ionic silver in parsley samples by means of direct HR-CS SS GFAAS by applying a newly introduced concept of evaluating atomization delay (t_{ad}) [31]. The most important parameters that influence t_{ad} were found to be atomization temperature, atomization heating rate and pyrolysis temperature. However, the applied multivariate approach in the above-mentioned previous study covered only small ranges for these variables. Therefore, as a first step in this study, broader temperature and heating rate ranges were investigated in order to find optimum conditions for discrimination of AgNPs from ionic Ag. Instead of a 3^3 factorial experimental design here, values 6, 9 and 14 for the respective parameter were tested in a multifactorial approach (see Electronic Supplementary Material Table S2). Optimum condition was defined as a compromise between maximum Δt_{ad} and lowest uncertainty as derived from the combined standard deviation of the replicate measurements. Figure 1 presents the results of these experiments obtained for a fixed pyrolysis temperature of 300 °C when investigating Ag-spiked parsley samples.

A clear trend for higher Δt_{ad} was found with decreasing atomization temperatures and rates. Taking into account the resulting uncertainty, an atomization temperature of 900 °C and an atomization heating rate of 1200 °C s^{-1} were selected as optimum with Δt_{ad}=1.08±0.28 s. Furthermore, the optimization of pyrolysis temperature was performed. Adjusting the pyrolysis temperature is particularly important when considering different matrix compositions of the food samples. Therefore, here three different matrices, namely parsley, apple and pasta, were used in order to evaluate whether a general trend can be observed and if setting a defined value will be feasible to investigate a variety of matrices. The obtained results for varying pyrolysis temperature from 250 to 700 °C in regard to Δt_{ad} and u_c are presented in Fig. 2.

Δt_{ad} values ranged between −0.77 and 1.39 s for the selected parameters and sample matrices. The fact that for pasta, t_{ad} for AgNPs is higher than that for Ag^+ when applying pyrolysis temperatures below 400 °C is striking and must be attributed to different interactions of Ag species with the matrix compared to apple or parsley matrix. This issue was further investigated and will be discussed below. However, as a general trend, highest $|\Delta t_{ad}|$ was observed for lower pyrolysis temperatures in all three tested matrices. Application of pyrolysis temperatures higher than 400 °C resulted in insignificant differences due to lower Δt_{ad} values compared to their combined uncertainty. Especially for apple, the increasing uncertainty with rising pyrolysis temperature is obvious (Fig. 2b). Therefore, the following experiments were conducted by selecting a constant optimum pyrolysis temperature of 250 °C. The resulting 3D atomic absorption signals for parsley, apple and pasta (see Electronic Supplementary Material Fig. S2) indicate that despite this very low pyrolysis

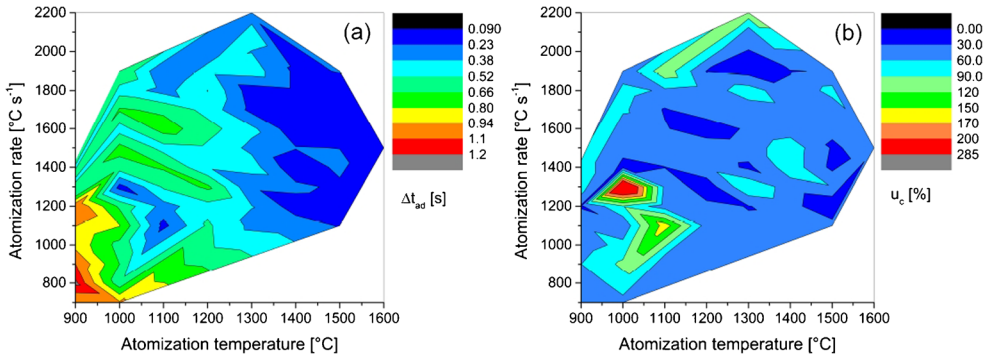

Fig. 1 (**a**) Mean values for difference in atomization delay (Δt_{ad}) (with $n=3$) and (**b**) relative combined uncertainty (u_c) depending on atomization temperature and atomization heating rate at a constant pyrolysis temperature of 300 °C. Atomization temperatures <850 °C and atomization rates <700 °C s^{-1} were not taken into account due to resulting incomplete atomization and high atomization times, respectively

temperature, background correction by iterative baseline correction is suitable to obtain reproducible and well-defined peaks without any severe interference from other elements or molecules.

Another parameter that was identified to influence atomization delays in this direct solid sampling measurement procedure was sample weight [31]. However, since the furnace parameters (atomization temperature, heating rate and pyrolysis temperature) were now significantly shifted towards lower values, this was again investigated with the new set of parameters for the three different matrices. The evaluation criteria for optimum sample weight were again defined as maximum Δt_{ad} in combination with minimum uncertainty in order to achieve significant discrimination of AgNPs from Ag^+. The results for sample weights varying from 0.1 to 0.4 mg are depicted in Fig. 3. Lowest tested sample weights of 0.1 mg result in very high uncertainties, which in the case of apple and pasta gave insignificant differences in t_{ad} values; i.e. Δt_{ad} was smaller than u_c. Most probably the micro-inhomogeneity of the samples becomes critical at this low mass aliquot [36, 37]. However, above 0.1 mg, the observed trends allow again setting an optimum value for all three matrices. With increasing sample weights, higher Δt_{ad} values were obtained and u_c decreased up to 0.2 mg, where optimal and significant values were achieved.

In summary, an atomization temperature of 900 °C at a heating rate of 1200 °C s^{-1} and a pyrolysis temperature of 250 °C were applied for a 0.2-mg sample aliquot introduced into the SS tube.

Homogeneity test for Ag-spiked food samples

One of the biggest difficulties involved in direct solid sampling analysis is the micro-inhomogeneity of the analyzed samples at sub-microgram weights [32, 38]. Hence, there is a need to ensure homogeneous distribution of the Ag spikes in the 18 self-prepared simulated foodstuff samples investigated in this study. For this purpose, the homogeneity factor was determined for all samples by applying four aliquots of approximately 0.2 mg of each sample and using the optimized furnace programme for AAS measurement. The relative standard deviations (RSDs) of the obtained signal intensities

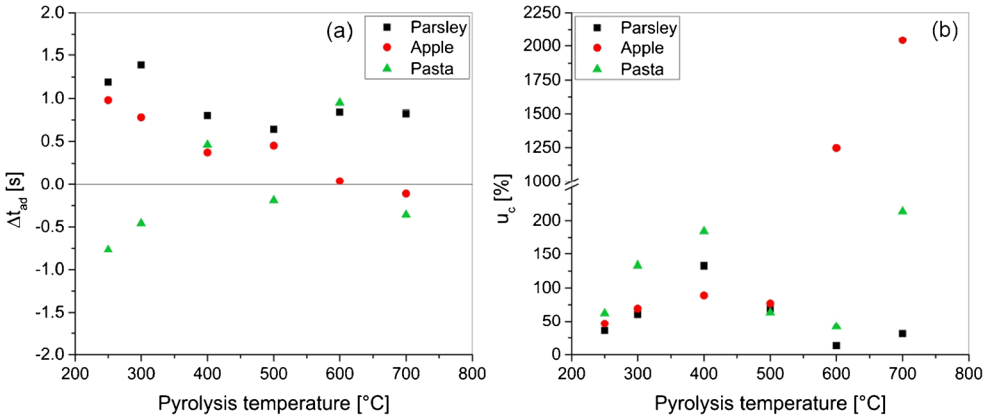

Fig. 2 (**a**) Mean values of difference in atomization delay (Δt_{ad}) (with $n=3$) and (**b**) relative combined uncertainty (u_c) depending on pyrolysis temperature received for parsley (*black square*), apple (*red circle*) and pasta (*green triangle*) at a constant heating rate of 1200 °C s^{-1} and an atomization temperature of 900 °C. Pyrolysis temperatures <250 °C were not taken into account because of strong matrix effects from inadequately matrix degradation ($n=3$)

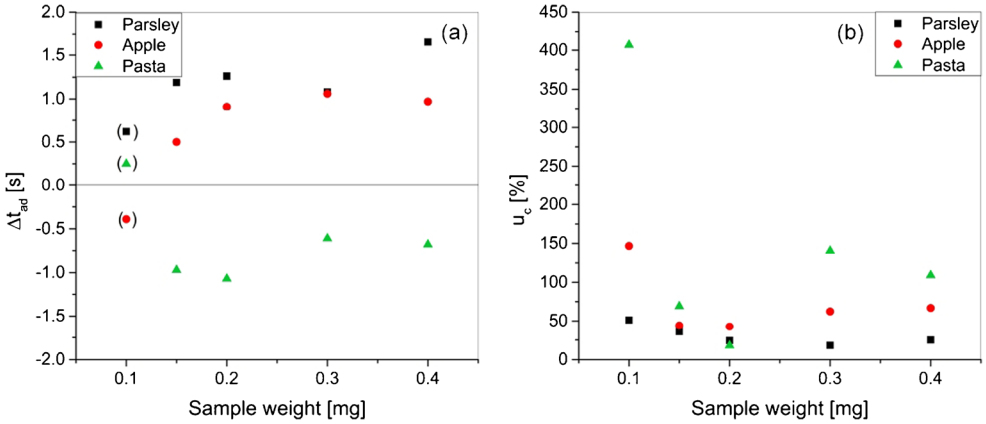

Fig. 3 (**a**) Mean values of difference in atomization delay Δt_{ad} (with n= 3) and (**b**) relative combined uncertainty (u_c) depending on sample weight received for parsley (*black square*), apple (*red circle*) and pasta (*green triangle*). Δt_{ad} values in *parentheses* in (**a**) are not significant differences in t_{ad} due to high uncertainties. Sample weights <0.1 and >0.5 mg were not studied due to difficulties in handling very small amounts and obtaining broad peak maxima, respectively. Furnace parameters are atomization temperature of 900 °C, atomization heating rate of 1200 °C s^{-1} and pyrolysis temperature of 250 °C

(absorbance) varied between 3 and 20 %. The relative homogeneity factors were calculated on the basis of RSDs using Eq. (1) and ranged from 1.43 % $mg^{1/2}$ for pepper samples to a maximum of 9.01 % $mg^{1/2}$ for cheese spiked with AgNPs. (A list for all 18 samples is provided in Electronic Supplementary Material Table S3.) Hence, all values were below 10 % $mg^{1/2}$ revealing acceptable homogeneity according to Kurfürst et al. [32].

Method application to food samples

The developed and optimized method was then applied to different food samples in order to prove if it is valid for diverse food matrices. As a first series of samples, eight food products, namely, apple, cheese, maize meal, onion, parsley, pasta, pepper and wheat flour, were spiked with either Ag^+ or AgNPs and examined using the proposed method. Secondly, mussel samples obtained from an exposure experiment with either Ag^+ or AgNPs were investigated. Finally, contact samples, i.e. pepper samples that were stored in AgNP-containing boxes for 7 days, were studied. As a first evaluation step, t_{ad} values were measured and compared for all samples (see Fig. 4a).

For food samples spiked with Ag^+, the t_{ad} values ranged from 11.31±0.29 s (apple) to 23.28±0.53 s (cheese), indicating different retentions of Ag^+ in these matrices. Nevertheless, similar product classes show comparable atomization delays, as can be seen especially for pasta, wheat flour and maize meal, containing carbohydrates as basic composition. Tissues of animal origin with high protein contents, like cheese and mussel, better retain Ag, which results in higher t_{ad}. Probably, the provision of functional groups, like mercapto or amine groups, in proteins and the high affinity of silver towards these

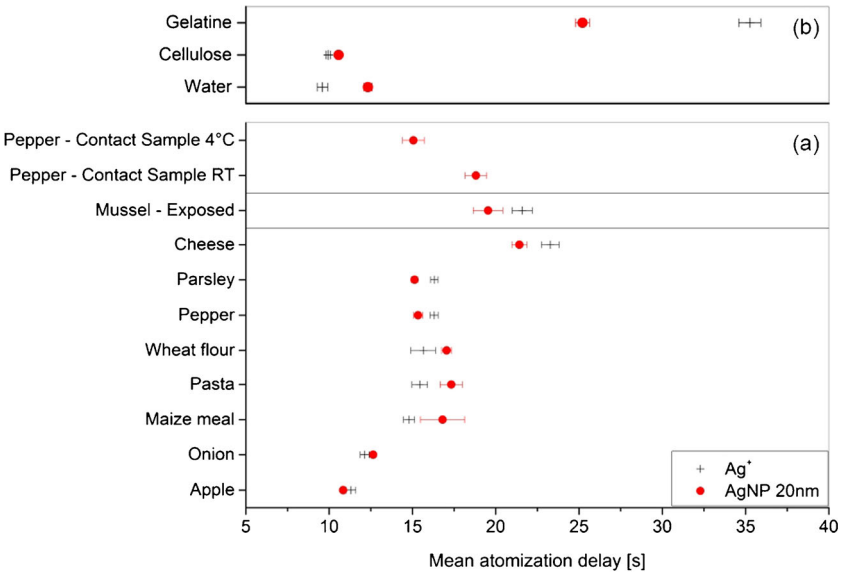

Fig. 4 Mean atomization delays (t_{ad}) for (**a**) food samples and (**b**) model matrices spiked with/exposed to ionic silver (*black plus*) and 20-nm AgNPs (*red circle*) obtained by application of the optimized furnace programme. *Error bars* represent ±1 SD from replicate measurements, n≥4

groups cause this behaviour. In order to support this theory, three model samples were prepared to simulate (a) carbohydrate matrix by cellulose, the main component of plant matter; (b) protein matrix using gelatine as polypeptide with high collagen content; and (c) water simulating lowest possible matrix interaction. As can be seen from Fig. 4b, the obtained values confirm this hypothesis. Moreover, the correlation between t_{ad} and matrix composition becomes obvious when taking into account the average carbohydrate/protein content (according to [39]) of the investigated food samples (see Fig. 5).

It is obvious that with increasing carbohydrate content in the matrices, the corresponding atomization delay decreased whereas rising protein content leads to increased atomization delay. However, the observed trends were less pronounced for AgNP-spiked samples compared to Ag^+-spiked samples. This suggests, as expected, that ionic silver interacts stronger with the matrix than AgNPs. In conclusion, these results evidence that matrix composition plays an important role in the atomization behaviour of the silver species. As a first conclusion, it is obvious though that valid application of the newly developed method requires reference measurement of an individual sample matrix spiked with Ag^+ in order to classify the matrix and reveal expected t_{ad} and Δt_{ad} values. This preliminary experiment can be seen as a kind of *one point calibration* of the suggested qualitative method.

Regarding the exposure samples, i.e. mussel tissue deriving from an exposure study with PVP-coated 75-nm AgNPs or $AgNO_3$, respectively, the respective atomization delays agree very well with the above-given explanations. Moreover, the significant lower t_{ad} for mussels exposed to AgNPs suggests that silver had been taken up in nanoparticulate form by the mussels and is still present in this form in the tissue. Future studies will address this hypothesis in more detail.

Concerning the two contact samples, it is first of all important to remark that a significant amount of silver had been transferred from the boxes' surfaces into the fresh pepper without addition of any auxiliary liquid or reagent during the experiment. The resulting concentrations were approximately 0.07 μg Ag g^{-1} of dried pepper. However, even though all the samples were exposed to AgNP-containing boxes, significantly different t_{ad} values were obtained. We suggest that AgNPs transferred to the pepper pulp, which was kept for 7 days at room temperature, were subject to oxidation due to deterioration of the pepper fruit and, hence, were detected as Ag^+. However, at 4 °C, such a process was prevented and AgNPs were still present (Pictures of the contact samples are provided in the Electronic Supplementary Material Fig. S3). REM investigations of the pepper samples were therefore performed in order to have further indication of this hypothesis.

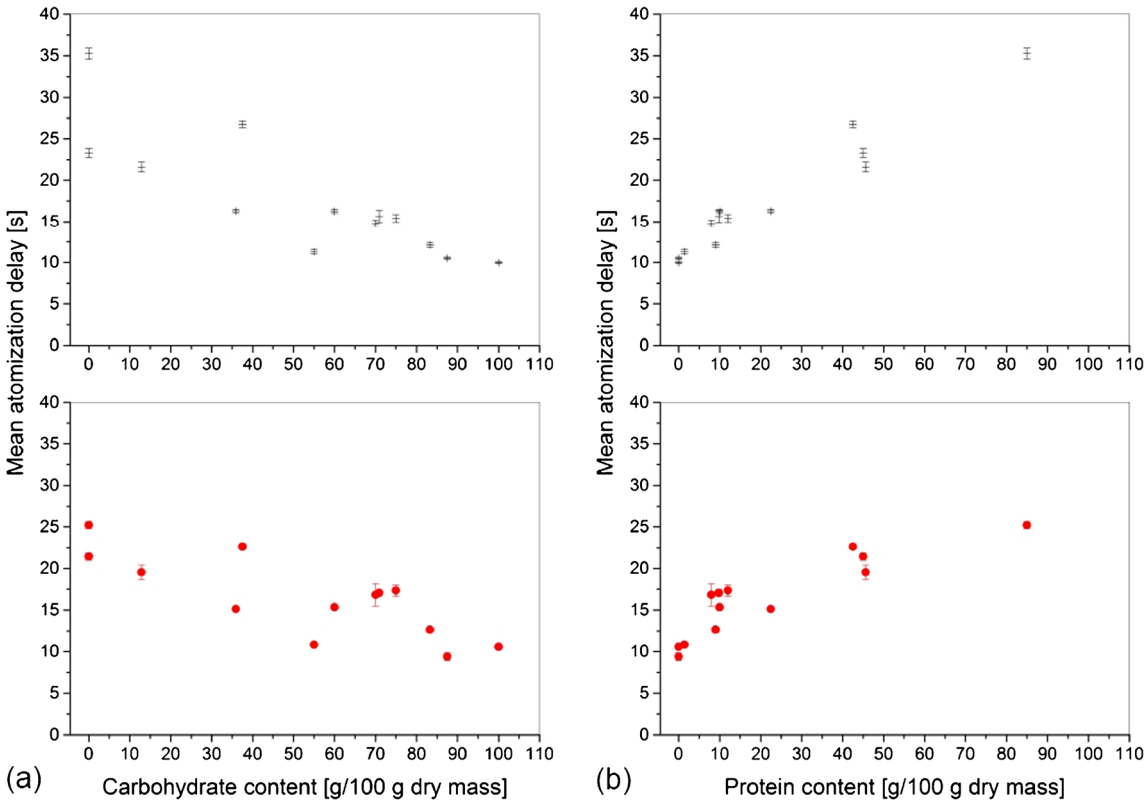

Fig. 5 Mean atomization delays for food samples and model matrices sorted by (**a**) average carbohydrate and (**b**) average protein content (according to [39]) of the investigated food samples. *Red circles* indicate AgNP-spiked samples, and *black crosses* indicate ionic Ag-spiked samples. *Error bars* represent uncertainty as derived from combined SD with $n \geq 4$

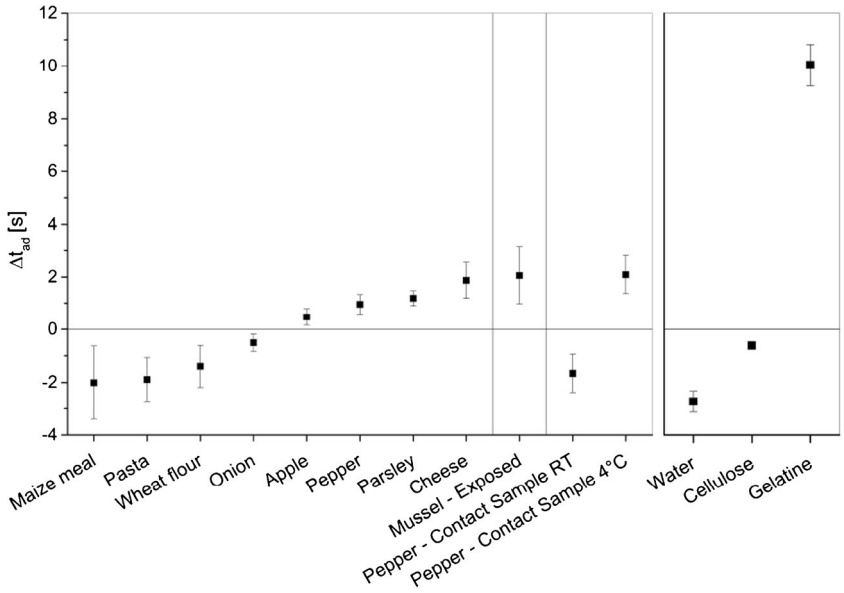

Fig. 6 Mean differences in atomization delays for food samples and model matrices. *Error bars* represent uncertainty as derived from combined SD with $n \geq 4$

However, the AgNPs could not be visualized in any of the samples due to the low concentration of silver in the samples.

Anyway, the detection and identification of AgNPs in a food sample is supposed to be evaluated by the difference in t_{ad}, i.e. by a significant Δt_{ad} value. Figure 6 presents the obtained Δt_{ad} values, which were all significant, i.e. allow discrimination of Ag^+-containing samples from AgNP-containing samples.

By far, the highest difference in t_{ad} (Δt_{ad}=10.04±0.78 s) was observed in gelatine matrix. Here, Ag^+ ions are retained much longer than AgNPs. In very good agreement with this finding, second highest values were obtained in high-protein samples, i.e. cheese and mussel. Lowest Δt_{ad} gave as expected water matrix (Δt_{ad}=−2.73±0.4 s). Here, it simply takes more time to atomize (large) AgNPs than to evaporate distributed (small) Ag^+ ions since no interaction with any matrix can occur. Similar behaviour showed pasta, wheat flour and maize meal, followed by cellulose matrix. In between were apple, pepper and parsley samples, where retention of Ag^+ ions by the matrix prevails over kinetic aspects of AgNP atomization, resulting in slightly positive Δt_{ad} values. No significant different was observed when comparing Ag^+-spiked pepper with the contact sample kept at RT. This result indicates the absence of nanoparticulate Ag, while Ag^+ ions were found. Hence, here again, the result is true when taking for granted the above-discussed theory of degradation of AgNPs to Ag^+ ions during this experiment.

In conclusion, the applicability of the suggested approach could be proven for all investigated biological matrices, since Ag^+ ions always showed significantly different atomization

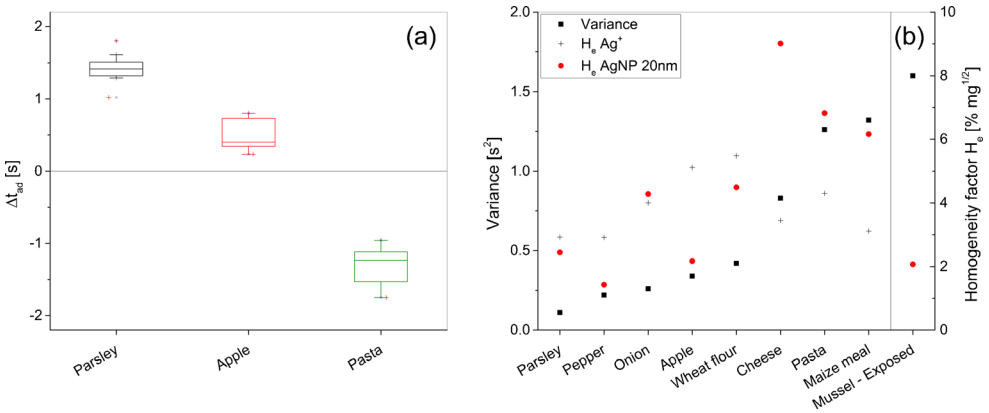

Fig. 7 Reproducibility of Δt_{ad} values when using several sample carriers and graphite tubes. (**a**) Δt_{ad} values and variation range for parsley, apple and pasta spiked with AgNP or Ag^+, respectively, when using 10 individual sample carriers. *Box plots* represent median values with $n \geq 40$. *Bars* give minimum and maximum value excluding outliers marked as *red crosses* (replicate measurements n=4; solid sampling platforms n=10). (**b**) Variances (σ^2) for Δt_{ad} values and homogeneity factors (H_e) of biological samples spiked with or exposed to AgNP or Ag^+, respectively, when using 4 individual sample carriers and graphite tubes ($n \geq 16$; replicate measurements $n \geq 4$; solid sampling platforms and graphite tubes n=4)

delays than AgNPs. However, as stated above, a kind of one point calibration, i.e. a reference measurement of the individual sample matrix spiked with Ag^+ is required prior to analysis of unknown samples. Consequently, it is important to investigate the influence of instrumental parameters on the validity of such calibration. Therefore, reproducibility tests with different sample carriers and graphite tubes on different days were performed.

Reproducibility tests

In a first series of experiments, the reproducibility of the proposed method was tested by replicate measurements of spiked parsley, apple and pasta samples with 10 individual solid sampling platforms of the same type. The results (Δt_{ad}) of this experiment are shown in Fig. 7a. For parsley, Δt_{ad} ranged from 1.29 to 1.61 s whereas the distribution of data for pasta was found to be between −0.96 and −1.75 s. This broader variation may derive from a higher sample inhomogeneity of 6.82 % $mg^{1/2}$ for pasta in comparison to 2.44 % $mg^{1/2}$ for parsley (see Electronic Supplementary Material Table S3). The median Δt_{ad} value for apple was relatively low (Δt_{ad}= 0.40 s), but due to the corresponding low variation, still significant difference was obtained, i.e. valid distinction between ionic silver and nanoparticulate silver was achieved. Hence, reproducible and valid results were obtained for the tested solid samples even when using 10 individual sample carriers.

In another series of experiments, the reproducibility was tested with more sample matrices and exchanging graphite tubes as well as sampling platforms. However, here, a lower number of replicates were used. The variances (σ^2) of Δt_{ad} values clearly depend on the matrix (see Fig. 7b) and, hence, must therefore be ascribed to sample homogeneity or matrix effects and not to instrumental parameters like apparatus drift or variations in graphite carriers and tubes. Correlation of homogeneity factor (H_e) and variance is obvious as highest σ^2 values were achieved for pasta and maize meal which had lowest homogeneity.

Nevertheless, replicate measurement with different solid sampling platforms and graphite tubes on several days still allows distinction of AgNPs from Ag^+ since the differences in t_{ad} were always significant.

Conclusions and outlook

This work addresses the urgent need to provide robust screening methods for the detection of silver nanoparticles in complex biological matrices that have to be investigated in e.g. food and eco-monitoring studies. A simple, fast and reliable procedure for the discrimination of AgNPs from ionic silver in biological samples is proposed using direct solid sampling HR-CS GFAAS omitting time-consuming sample pre-treatment. A previously introduced approach that suggests the evaluation of atomization delays (t_{ad}) in GFAAS in order to detect AgNPs in solid parsley was further developed and applied to a broad variety of biological matrices. These include tissues of animal origin, like mussel and cheese, as well as samples deriving from exposure and contact studies with AgNPs. In all nine investigated matrices (parsley, apple, pepper, cheese, onion, pasta, maize meal, wheat flour and mussel), 20-nm AgNPs were identified and discriminated from Ag^+ ions due to significantly different t_{ad} values using the same optimized furnace programme. Δt_{ad} values varied from −2.01 s for maize meal to +2.06 s for mussel tissue. The robustness and reproducibility of the method were approved with regard to sufficient homogeneity of the micro samples applied for solid sampling and also regarding instrumental parameters such as individual graphite tubes and platforms as well as measurements on different days.

The observed influence of the matrix composition on t_{ad} was more pronounced for Ag^+-spiked samples than for AgNP-containing samples, revealing a stronger interaction of the ions with the matrix components. Clear trends, i.e. decreasing t_{ad} with increasing carbohydrate content and inverse trend for protein content, were found and confirmed by investigation of cellulose and gelatine as model samples. These findings give first insights in the involved mechanisms; however, future studies are planned to further elucidate this issue.

Acknowledgments The authors are very grateful to Deutsche Forschungsgemeinschaft for their financial support of this work by project LE 2457/8-1.

Compliance with ethical standards

Conflict of interest The authors declare that they have no competing interests.

References

1. Duncan TV (2011) Applications of nanotechnology in food packaging and food safety: barrier materials, antimicrobials and sensors. J Colloid Interface Sci 363:1–24. doi:10.1016/j.jcis.2011.07.017
2. Chaudhry Q, Scotter M, Blackburn J, Ross B, Boxall A, Castle L, Aitken R, Watkins R (2008) Applications and implications of nanotechnologies for the food sector. Food Addit Contam Part A 25: 241–258. doi:10.1080/02652030701744538
3. Jokar M, Rahman RA (2014) Study of silver ion migration from melt-blended and layered-deposited silver polyethylene nanocomposite into food simulants and apple juice. Food Addit Contam Part A
4. von Goetz N, Fabricius L, Glaus R, Weitbrecht V, Günther D, Hungerbühler K (2013) Migration of silver from commercial plastic food containers and implications for consumer exposure assessment. Food Addit Contam Part A 30:612–620

5. Artiaga G, Ramos K, Ramos L, Cámara C, Gómez-Gómez M (2015) Migration and characterisation of nanosilver from food containers by AF4-ICP-MS. Food Chem 166:76–85. doi:10.1016/j.foodchem.2014.05.139
6. Addo Ntim S, Thomas TA, Begley TH, Noonan GO (2015) Characterization and potential migration of silver nanoparticles from commercially available polymeric food contact materials. Food Addit Contam Part A
7. Echegoyen Y, Nerín C (2013) Nanoparticle release from nanosilver antimicrobial food containers. Food Chem Toxicol 62:16–22. doi:10.1016/j.fct.2013.08.014
8. Cushen M, Kerry J, Morris M, Cruz-Romero M, Cummins E (2014) Evaluation and simulation of silver and copper nanoparticle migration from polyethylene nanocomposites to food and an associated exposure assessment. J Agric Food Chem 62:1403–1411. doi:10.1021/jf404038y
9. Cushen M, Kerry J, Morris M, Cruz-Romero M, Cummins E (2013) Migration and exposure assessment of silver from a PVC nanocomposite. Food Chem 139:389–397. doi:10.1016/j.foodchem.2013.01.045
10. Jany AK, Kuiper H, Larsen JC, Le Neindre P, Schans J, Schlatter J, Silano V, Skerfving S, Vannier P (2009) Scientific opinion of the Scientific Committee on a request from the European Commission on the Potential Risks Arising from Nanoscience and Nanotechnologies on Food and Feed Safety. EFSA J 958:1–39
11. EFSA Panel on Food Contact Materials, Enzymes, Flavourings and Processing Aids (CEF) (2011) Scientific opinion on the safety evaluation of the substance, silver zeolite A (silver zinc sodium ammonium aluminosilicate), silver content 2-5 %, for use in food contact materials. EFSA J 9:1999–2011
12. (2011) Verordnung (EU)Nr. 1169/2011 des Europäischen Parlaments und des Rates. 1–46
13. (2011) Commission recommendation of 18 October 2011 on the definition of nanomaterial. 1–3
14. Lövestam G, Rauscher H, Roebben G, Klüttgen BS, Gibson N, Putaud J-P, Stamm H (2010) Considerations on a definition of nanomaterial for regulatory purposes. Publications Office
15. Wigginton NS, Haus KL, Hochella MF Jr (2007) Aquatic environmental nanoparticles. J Environ Monit 9:1306–1316. doi:10.1039/b712709j
16. Tiede K, Boxall ABA, Tiede D, Tear SP, David H, Lewis J (2009) A robust size-characterisation methodology for studying nanoparticle behaviour in "real" environmental samples, using hydrodynamic chromatography coupled to ICP-MS. J Anal At Spectrom 24:964–972. doi:10.1039/b822409a
17. Blasco C, Picó Y (2011) Determining nanomaterials in food. Trends Anal Chem 30:84–99. doi:10.1016/j.trac.2010.08.010
18. Farré M, Sanchís J, Barceló D (2011) Analysis and assessment of the occurrence, the fate and the behavior of nanomaterials in the environment. Trends Anal Chem 30:517–527. doi:10.1016/j.trac.2010.11.014
19. Silva BFD, Pérez S, Gardinalli P, Singhal RK, Mozeto AA, Barceló D (2011) Analytical chemistry of metallic nanoparticles in natural environments. Trends Anal Chem 30:528–540. doi:10.1016/j.trac.2011.01.008
20. Justino CIL, Rocha-Santos TA, Duarte AC (2011) Sampling and characterization of nanoaerosols in different environments. Trends Anal Chem 30:554–567. doi:10.1016/j.trac.2010.12.002
21. Domingos RF, Baalousha MA, Ju-Nam Y, Reid MM, Tufenkji N, Lead JR, Leppard GG, Wilkinson KJ (2009) Characterizing manufactured nanoparticles in the environment: multimethod determination of particle sizes. Environ Sci Technol 43:7277–7284. doi:10.1021/es900249m
22. Bolea E, Jiménez-Lamana J, Laborda F, Abad-Álvaro I, Bladé C, Arola L, Castillo JR (2014) Detection and characterization of silver nanoparticles and dissolved species of silver in culture medium and cells by AsFlFFF-UV-Vis-ICPMS: application to nanotoxicity tests. Analyst 139:914–922. doi:10.1039/C3AN01443F
23. Loeschner K, Navratilova J, Købler C, Mølhave K, Wagner S, von der Kammer F, Larsen EH (2013) Detection and characterization of silver nanoparticles in chicken meat by asymmetric flow field flow fractionation with detection by conventional or single particle ICP-MS. Anal Bioanal Chem 405:8185–8195. doi:10.1007/s00216-013-7228-z
24. Cascio C, Geiss O, Franchini F, Ojea-Jimenez I, Rossi F, Gilliland D, Calzolai L (2015) Detection, quantification and derivation of number size distribution of silver nanoparticles in antimicrobial consumer products. J Anal At Spectrom 30:1255–1265. doi:10.1039/C4JA00410H
25. Mitrano DM, Lesher EK, Bednar A, Monserud J, Higgins CP, Ranville JF (2012) Detecting nanoparticulate silver using single-particle inductively coupled plasma-mass spectrometry. Environ Toxicol Chem 31:115–121. doi:10.1002/etc.719
26. Linsinger TPJ, Peters R, Weigel S (2014) International interlaboratory study for sizing and quantification of Ag nanoparticles in food simulants by single-particle ICPMS. Anal Bioanal Chem 406:3835–3843. doi:10.1007/s00216-013-7559-9
27. Gagné F, Turcotte P, Gagnon C (2012) Screening test of silver nanoparticles in biological samples by graphite furnace-atomic absorption spectrometry. Anal Bioanal Chem 404:2067–2072. doi:10.1007/s00216-012-6258-2
28. Resano M, Aramendía M, Belarra MA (2014) High-resolution continuum source graphite furnace atomic absorption spectrometry for direct analysis of solid samples and complex materials: a tutorial review. J Anal At Spectrom 29:2229–2250. doi:10.1039/C4JA00176A
29. Resano M, Lapeña AC, Belarra MA (2013) Potential of solid sampling high-resolution continuum source graphite furnace atomic absorption spectrometry to monitor the Ag body burden in individual Daphnia magna specimens exposed to Ag nanoparticles. Anal Methods 5:1130–1139. doi:10.1039/c2ay26456k
30. Resano M, Mozas E, Crespo C, Briceño J, del Campo Menoyo J, Belarra MA (2010) Solid sampling high-resolution continuum source graphite furnace atomic absorption spectrometry to monitor the biodistribution of gold nanoparticles in mice tissue after intravenous administration. J Anal At Spectrom 25:1864–1873. doi:10.1039/c0ja00086h
31. Feichtmeier NS, Leopold K (2014) Detection of silver nanoparticles in parsley by solid sampling high-resolution–continuum source atomic absorption spectrometry. Anal Bioanal Chem 406:3887–3894. doi:10.1007/s00216-013-7510-0
32. Kurfürst U, Pauwels J, Grobecker K-H, Stoeppler M, Muntau H (1993) Micro-heterogeneity of trace elements in reference materials—determination and statistical evaluation. Fresenius J Anal Chem 345:112–120
33. Osterauer R, Marschner L, Betz O, Gerberding M, Sawasdee B, Cloetens P, Haus N, Sures B, Triebskorn R, Köhler H-R (2010) Turning snails into slugs: induced body plan changes and formation of an internal shell. Evol Dev 12:474–483. doi:10.1111/j.1525-142X.2010.00433.x
34. Greulich C, Diendorf J, Simon T, Eggeler G, Epple M, Köller M (2011) Uptake and intracellular distribution of silver nanoparticles in human mesenchymal stem cells. Acta Biomater 7:347–354. doi:10.1016/j.actbio.2010.08.003
35. Sures B, Zimmermann S (2007) Impact of humic substances on the aqueous solubility, uptake and bioaccumulation of platinum, palladium and rhodium in exposure studies with Dreissena polymorpha. Environ Pollut 146:444–451. doi:10.1016/j.envpol.2006.07.004
36. da Silva AF, Borges DLG, Lepri FG, Welz B, Curtius AJ, Heitmann U (2005) Determination of cadmium in coal using solid sampling

graphite furnace high-resolution continuum source atomic absorption spectrometry. Anal Bioanal Chem 382:1835–1841. doi:10.1007/s00216-005-3327-9

37. Welz B, Vale MGR, Borges DLG, Heitmann U (2007) Progress in direct solid sampling analysis using line source and high-resolution continuum source electrothermal atomic absorption spectrometry. Anal Bioanal Chem 389:2085–2095. doi:10.1007/s00216-007-1555-x
38. Baysal A, Akman S (2010) Determination of lead in hair and its segmental analysis by solid sampling electrothermal atomic absorption spectrometry. Spectrochim Acta B At Spectrosc 65:340–344. doi:10.1016/j.sab.2010.02.016
39. United States Department of Agriculture, Agricultural Research Service (2015) National Nutrient Database for Standard Reference Release 27. In: Nutr. List. http://ndb.nal.usda.gov/ndb/nutrients/index. Accessed 20 Aug 2015